MATHEMATICAL MODELING AND NUMERICAL SIMULATION OF A REFRIGERATION CONDENSER IN DYNAMIC REGIME

Achour MANSOURI [1, *], Hamou SOUALMI [2], Ahmed HAIDOUR [3], Boumediene TOUATI [4], Farouk MEGUELLATI [5]

This work is consecrated to the mathematical modeling and numerical simulation of the flow of an R-22 refrigerant inside the horizontal circular tubes of the coil of a compact finned-tube condenser in dynamic regime. The system of equations governing the flow in the two-phase region consists of six equations and, three equations in the single-phase region. These equations are of hyperbolic type with source terms. Moreover, two equations: one is the energy equation applied to the air and the other is the energy equation applied to the wall of the coil tube. The equations are discretized using the finite difference method, and the resolution of this system was completed using the Newton-Raphson method. The results obtained from the simulation allow for the prediction of the evolution of the thermophysical properties of the refrigerant and the temperatures of the coil tube wall and the air along the condenser tube. These results are consistent in terms of profile with other works found in the literature.

Keywords: Simulation, modeling, two-phase, flow, condenser, refrigerant, dynamic regime, fins.

1. Introduction

Air cooler condensers are generally tubular heat exchangers, and the tubes used are quite thin and triangular or square in arrangement. They allow heat to be transferred between two fluids with different temperatures through a wall. Usually, these tubes are connected with rounded base fins whose purpose is to increase the heat transfer to the outside. While the performance of these condensers is a key

* Corresponding author
[1] Doctor Research Unit for Renewable Energies in Saharan Region, URERMS, Renewable Energy Development Center, Adrar, Algeria, mansouri_achour@yahoo.fr
[2] Doctor Research Unit for Renewable Energies in Saharan Region, URERMS, Renewable Energy Development Center, Adrar, Algeria, soualmi_hamou@yahoo.fr
[3] Student, University TAHRI Mohammed Bechar, Faculty of Technology, Laboratory for Energy in Arid Zones (ENERGARID), Algeria, haidour.ahmed@univ-bechar.dz
[4] Prof., University TAHRI Mohammed Bechar, Faculty of Technology, Laboratory for Energy in Arid Zones (ENERGARID), Algeria, btouatidz@yahoo.fr
[5] Researcher, Research Unit for Renewable Energies in Saharan Region, URERMS, Renewable Energy Development Center, Adrar, Algeria, farouksdz@yahoo.fr

factor in the thermal design of refrigeration systems, improvements in modeling are essential for better prediction of their performance. However, their study presents complexities that arise from:

- During the flow of refrigerant in the circuit, it undergoes several phase changes (superheated, vapor-mixture, liquid);
- Their complex geometric configuration;

Although the equations governing the physical phenomenon can be formulated, due to these complexities, there are several modeling approaches, but the choice depends on a compromise between the accuracy of the results and the complexity of the chosen model. A technical classification of modeling has been introduced in recent years and can be subdivided as follows:

- The method of displacement of the boundaries of the dependent phases;
- The method of finite differences of the independent phases;

The first method consists of subdividing the length of the condenser tube into three segments, and each segment presents a single state of the refrigerant (superheated vapor, mixture or liquid). In the present study, the condenser is modeled in three zones with a simple and deterministic approach, and this approach is illustrated in the works of Cristian Cuevas, Jean Lebrun et al. [1], M. Willatzen, N.B.O.L. Pettit et al. [2, 3] and Xing Xuea, Xianming Fenga et al. [4]. While the second method (finite differences), the equations governing the flow are described by a scheme in which the length of the condenser is divided into a multitude of identical finite volume elements. Each element is defined by its own state properties; therefore, the mathematical formulation of an element for a given phase is not valid for the other two phases. In literature, we find various works devoted to this study, among them X. Jia, C. P. Tso et al. [5], H. Wang and S. Touber [6] and F.Q. Wang, G.G. Maidmentet et al. [7]. This method is used in this work where the flow configuration is considered annular and the pressures of the two liquid and vapor phases are different. The transition point between the superheated vapor/mixture and mixture/liquid phases is predicted using the Vandermonde matrix method [8] whose aim is to accurately determine the transition point between the states of the fluid. In this study, the condenser is modeled in three zones, using a "deterministic" approach [1]. The geometry of the condenser is known and the heat transfer coefficients, the void fraction, the pressure losses and the dynamic viscosity are calculated using correlations from the literature.

2. Mathematical modeling of the flow

During the flow of the refrigerant through the circuit tubes, the fluid undergoes several state changes, which are (see figures 1):

- Region of superheated vapor single-phase flow;
- Two-phase flow region (liquid-vapor);

- Region of liquid single-phase flow.

The different models of single-phase or two-phase flow are all based on the local mass conservation equations (continuity, momentum, energy) and are established as follows (see Fig. 2): We consider an infinitesimal control volume comprising two phases separated by an interface.

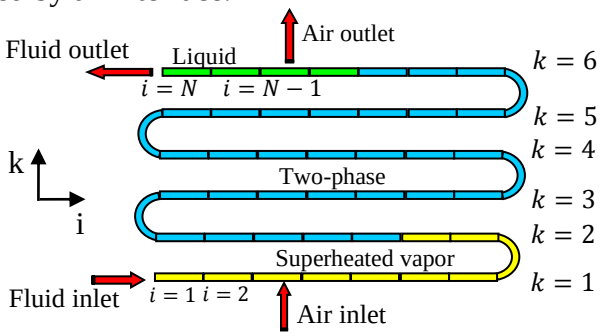

Fig. 1. The distribution of nodes along the coil of a condenser in the first stage [3].

In this volume, we write the mass, momentum, and energy balances for each phase. Subsequently, to solve these equations, a number of approximations must be assumed, and they are:

- The temperatures of the two phases are identical: $T = T_L = T_V$;
- The viscous diffusion terms (molecular and turbulent) are negligible;
- The tubes are assumed to be straight and horizontal, and the gravitational and interfacial forces are negligible;
- The mass flow rates transferred between the liquid Γ_L phase and the vapor phase Γ_V per unit volume are equal, but of opposite sign;
- The configuration of the mixed flow is annular.

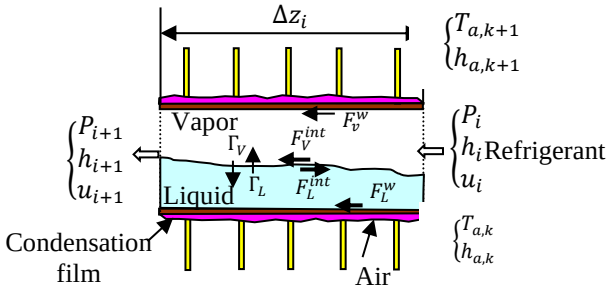

Fig. 2. Control volume.

The continuity equations for the liquid and vapor are [5, 9]:

$$\frac{\partial}{\partial t}[\rho_L(1-\alpha)] + \frac{\partial}{\partial z}\left(\rho_L U_L(1-\alpha)\right) - \Gamma_L = 0 \quad (1)$$

$$\frac{\partial}{\partial t}(\rho_V \alpha) + \frac{\partial}{\partial z}(\rho_V U_V \alpha) - \Gamma_V = 0 \quad (2)$$

The mass velocity G, the density ρ, and the average mixture enthalpy $\overline{h}$ can respectively be expressed as follows [9, 10]:

$$G = \frac{\alpha\rho_V U_V}{x} = \frac{(1-\alpha)\rho_L U_L}{(1-x)} \tag{3}$$

$$\rho = \alpha\rho_V + (1-\alpha)\rho_L \tag{4}$$

$$\overline{h} = \left[\rho_V \alpha h_V + \rho_L (1-\alpha) h_V\right]/\rho \ = (1-x)h_L + x h_V \tag{5}$$

Taking into account equation (4), equation (3) will become [5, 9]:

$$\frac{\partial\rho}{\partial t} + \frac{\partial(\rho U)}{\partial z} = 0 \tag{6}$$

The equations of momentum for the two phases are written as [6,9]:

$$\frac{\partial}{\partial t}\left[\rho_L U_L (1-\alpha)\right] + \frac{\partial}{\partial z}\left[\rho_L U_L^2 (1-\alpha)\right] = -(1-\alpha)\frac{\partial P}{\partial z} + \mathrm{F}_L^w \tag{7}$$

$$\frac{\partial}{\partial t}\left(\rho_V U_V \alpha\right) + \frac{\partial}{\partial z}\left(\rho_V U_V^2 \alpha\right) = -\alpha\frac{\partial P}{\partial z} + \mathrm{F}_V^w \tag{8}$$

The resultant of the friction forces between the wall and the two phases is [6]:

$$\mathrm{f}_x = \mathrm{F}_V^w + \mathrm{F}_L^w \tag{9}$$

This friction is expressed as a function of the two-phase multiplier and the pressure drop of a single phase, and is given by the following equation [6, 11]:

$$\mathrm{f}_x = \Phi_{ko}\left(-\frac{d\mathrm{P}}{d\mathrm{z}}\right)_{ko} \tag{10}$$

Similarly, the equation for the momentum of the mixture is the summation of equations (7) and (8) and, after some rearrangements, is written as follows [5, 9]:

$$\frac{\partial}{\partial t}(\rho U) + \frac{\partial}{\partial z}\left(\beta\rho U^2\right) = -\frac{\partial P}{\partial z} + \mathrm{f}_x \tag{11}$$

Where:

$$\beta = x^2\left[1 + \frac{(1-\alpha)\rho_L}{\alpha\rho_V}\right] + (1-x)^2\left[1 + \frac{(1-\alpha)\rho_V}{\alpha\rho_L}\right] \tag{12}$$

Applying the first law of thermodynamics to the control volumes of the liquid and vapor allowed the energy equations of each phase to be deduced. Similarly, the resulting mixing equation is the summation of the two balances of these two phases. [10, 11]:

$$\frac{\partial}{\partial t}\left(\rho\overline{h} + \frac{G^2}{2\rho'} - P\right) + \frac{\partial}{\partial z}\left\{G\overline{h} + G^3\left[\frac{x^3}{2\alpha^2\rho_V^2} + \frac{(1-x)^3}{2(1-\alpha)^2\rho_L^2}\right]\right\} = \frac{\pi D_i}{A_i}Q_w \tag{13}$$

Where [6,9]:

$$Q_w = h_r(T_w - T_r) \tag{14}$$

The term ρ' (sometimes called the momentum density) is defined as follows [10, 12]:

$$\rho' = \left[\frac{(1-x)^2}{\rho_L(1-\alpha)} + \frac{x^2}{\rho_V \alpha}\right]^{-1} \tag{15}$$

In the single-phase region, the situation is relatively simple, and the mass conservation equations are expressed as follows [6, 13]:

$$\frac{\partial \rho}{\partial t} + \frac{\partial(\rho U)}{\partial z} = 0 \tag{16}$$

$$\frac{\partial(\rho U)}{\partial t} + \frac{\partial\left(\rho U^2 + P\right)}{\partial z} = f_w \tag{17}$$

$$\frac{\partial(\rho h - P)}{\partial t} + \frac{\partial(\rho U h)}{\partial z} = \frac{\pi D_i}{A_i} Q_w \tag{18}$$

3. Energy equation applied to the tube wall

The energy equation applied to a finite length element of the tube wall is expressed as follows [6, 9]:

$$\mathrm{M}_w C_{p,w} \frac{\partial \mathrm{T}_w}{\partial t} = Q_a + Q_r \tag{19}$$

While the tubes and fins are generally made of different materials, the specific heat of the metal that is constituted is given as follows [6, 9]:

$$C_{p,w} = \frac{C_{p,tube}\mathrm{M}_{tube} + C_{p,ailette}\mathrm{M}_{ailette}}{\mathrm{M}_w} \tag{20}$$

4. Energy equation applied to air

In this work, we adopt the approach that the air is in a dry state and that the conduction between the fins is negligible. Therefore, the energy equation is [6, 14]:

$$\frac{d(\dot{m}_a h_a)}{dz_\kappa} = (\pi D_0) Q_a \tag{21}$$

The flux transferred by sensible heat is defined according to Wang [6, 14] by the following expression:

$$Q_a = \frac{\left(A_o + \eta_f A_f\right)}{\pi D_0 \Delta z_i} h_{a,s}(T_{to} - T_a) \tag{22}$$

The heat transfer coefficients are expressed in terms of the Colburn factor and are defined according to references [14, 15] as follows:

$$j_s = \frac{h_{a,s}}{G_a C_{p,a}} Pr_a^{2/3} \tag{23}$$

The efficiency of the cylindrical base fin is given according to H. Wang [6] by the following expression:

$$\eta_f = tgh\left\{0.5\left(\Delta z_j - D_0\right)\left(\frac{2\psi h_a}{K_f e_f}\right)^{0.5}\right\} \Big/ \left\{0.5\left(\Delta z_j - D_0\right)\left(\frac{2\psi h_a}{K_f e_f}\right)^{0.5}\right\} \tag{24}$$

Where: ψ is equal to 0.85 for the case of a cylindrical base fin.
The total efficiency of the dry finned surface can be formulated as follows [6, 15]:

$$\eta_{s,a} = 1 - \frac{A_f}{A_o}\left(1 - \eta_f\right) \tag{25}$$

The pressure losses inside a circular tube for a single-phase flow are given as follows [16]:

$$\Delta P = \frac{1}{2} f \rho \frac{U^2}{D_i} \tag{26}$$

Whereas, for a two-phase flow, we adopted the Mishima correlation [10, 16] which is expressed as follows:

$$\Delta P = \phi_{LO} \Delta P_{LO} \tag{27}$$

In this work, we adopted the geometric calculation methods cited in references [17, 18], and the friction factor is provided in reference [19].

5. The different correlation models used

In this study, we adopt Wallis's model (1969) [14] which is expressed as follows:

$$\alpha = \begin{cases} (1. + X_{TT}^{0.8})^{-0.378} & X_{TT} \leq 10. \\ 0.823 - 0.15 log(X_{TT}) & X_{TT} > 10. \end{cases} \tag{28}$$

The heat transfer coefficient between the refrigerant and the inner wall of the tube in the single-phase state is given by the formula below (vapor state $n = 0.3$, liquid state $n = 0.4$) [16, 20]:

$$h_r = 0.023 Re^{0.8} Pr^n \frac{K_r}{D_i} \tag{29}$$

While the heat transfer coefficient of a two-phase flow is given by the Akers correlation (1959) [10, 20]:

$$h_r = \begin{cases} 0.0265 \dfrac{k_L}{D_i} Re_{eq}^{0.8} Pr_L^{1/3} & Re_{eq} \geq 5 \times 10^4 \\ 5.03 \dfrac{k_L}{D_i} Re_{eq}^{0.8} Pr_L^{1/3} & Re_{eq} < 5 \times 10^4 \end{cases} \quad (30)$$

$$Re_{eq} = Re_{LO} + Re_{VO} \left(\frac{\mu_V}{\mu_L}\right) \left(\frac{\rho_L}{\rho_V}\right)^{0.5} \quad (31)$$

Re_{eq}: Reynolds number for an equivalent mass flow. The correlation for dynamic viscosity adopted in this work is that of McAdams [11].

6. Conditions of transition between zones

The transition between the three phases when the refrigerant flows through the condenser tubes is described by the enthalpy, pressure, and quality of the vapor as shown below [21]:

- The superheated vapor zone : if $h(P) > h_{V,sat}(P)$ and $x = 1$;
- The two-phase zone : if $h_{L,sat}(P) < h(P) < h_{V,sat}(P)$ and $0 < x < 1$;
- The liquid zone : if $h(P) < h_{L,sat}(P)$ et $x = 0$.

7. Newton-Raphson method

The Newton-Raphson method allows solving the systems of equations of the two-phase and single-phase flow models and finding the vector of unknowns $\vec{X} = \{\rho, U, T_r, T_w, T_a\}$ that satisfies the five functions $F_k(X_k)$ of multiple variables(ρ, U, T_r, T_w, T_a) in space $(i, j, k)$and time t [22]:

$$F_k(\rho, U, T_r, T_w, T_a)_k = 0 \quad (32)$$

For example, after discretizing the continuity equation using the finite difference method, it follows that:

$$F_1 = \left\{ \left[(\rho)_{i,j,k}\right]^{t+\Delta t} - \left[(\rho)_{i,j,k}\right]^{t} \right\} + \frac{\Delta t}{\Delta Z_i} \left\{ \left[(\rho U)_{i,j,k}\right]^{t+\Delta t} - \left[(\rho U)_{i-1,j,k}\right]^{t+\Delta t} \right\} \quad (33)$$

To predict the correction vector of the unknowns, we solve the nonlinear system indicated in matrix form as follows [22]:

$$J(X_k^0)\delta(X_k^0) = -F(X_k^0) \quad (34)$$

Where: $J(X_k^0) = \frac{\partial F_k(X_k^0)}{\partial X_k}$: designates the Jacobian matrix evaluated at the initial vector X_k^0, $\delta(X_k^0)$: correction vector, $F(X_k^0)$: residual vector evaluated at X_k^0 :

Solving the system of equations indicated by equation (34) allows us to obtain the roots of the first approximation of the solution of our system, and for the nth iteration, the new root values are written in the following compact form [22]:

$$X_k^{n+1} = X_k^n + \delta(X_k^n) \tag{35}$$

8. Initial and boundary conditions in the condenser

In a dynamic model, all thermophysical quantities are considered time-dependent, and the initial conditions have an impact on the performance of the system at start-up; therefore, this state plays an important role in the results obtained. Unfortunately, it is very difficult to track the initial distribution of these quantities along the serpentine tubes. For this purpose, the initial state is only based on the hypothesis that the fluid is in two-phase equilibrium or in a superheated state. In our study, it was assumed that the refrigerant is in the saturated vapor state and the initial conditions in the condenser are calculated at the vapor saturation temperature of the order of 30°C ($P_0 = 1.1919\ MPa$). In addition, at the boundary conditions at the inlet of the condenser, it was assumed that the isentropic compression efficiency is of order one (100%) with a temperature difference of 10°C between each time increment. The geometric and physical parameters of the condenser used in the numerical simulation are mentioned in Table 1.

Table 1. Geometric and physical parameters.

Symb.	Values	Designations
N	5	Number of equations
ND	10000	Number of nodes along the tube
t	0.3 mm	Fin thickness
S	2.3 mm	Space between two fins
n	6	Number of tubes per row
N	3	Number of tubes row
dz_i	10.mm	Dimension of the node in front of the flow
dz_j	50. mm	Dimension of the node along the vertical J
dz_k	50.mm	Dimension of the node according to face k
$\dot{m}$	25 Kg/h	Mass flow rate of refrigerant
T_{amb}	35°C	Ambient temperature
$R22$	/	Refrigerant
D_0	10. mm	Outside diameter of the tube
D_i	8. mm	Inner diameter of the tube
$C_{P,alim}$	0.86 KJ/kg.k	Specific heat of Aluminum
dt	0.5s	Time increment
X_{long}	25 m	The length of the heat exchanger
K_f	200W/m.k	Thermal conductivity of the aluminum fin.
K_{cuiv}	389 W/m.k	Thermal conductivity of copper
U_{air}	3 m/s	The air speed outside
ρ_{cuiv}	8940 Kg/m^3	Copper density
$C_{P,cuiv}$	0.38 KJ/kg.k	Specific heat of copper
ρ_{alum}	2700 g/m^3	Aluminum density

9. Methodology for numerical resolution of systems of equations

The system of equations to be solved in this work for each model (single-phase and two-phase) consists of five equations with five unknowns ($\boldsymbol{\rho_r, U, T_r, T_w, T_a}$). Such that, the single-phase model is formulated by equations (16), (17), (18), (19) and (21), and the two-phase model is constituted by equations (6), (11), (13), (19) and (21). Therefore, the resolution of these two systems of equations with several unknowns requires knowledge of the heat transfer coefficients and the pressure losses due to friction for each model, in addition to the void fraction and the vapor quality respectively for the two-phase model. By highlighting that the use of the subroutines of McLinden Refprop V7.0 [23] makes it possible to calculate all the thermodynamic quantities of the refrigerant if we know two quantities between them, and in our case, these are the temperature and the density. While the properties of the air are calculated with the correlations indicated in Ref. [24].

The methodology of the numerical solution of the global mathematical model mentioned previously involves the division of the condenser tube into small-sized cells. Each cell of a phase has five unknown variables $(\rho_r, U, T_r, T_w, T_a)$. For each cell, the flow is governed by differential equations that are easily discretized via the finite difference method, and this gives rise to a set of nonlinear, nonhomogeneous, and coupled equations (hyperbolic system of equations including source terms). Therefore, the five equations of each model must be formulated as follows: $F_i(\rho_i, u_i, T_{ri}, T_{pi}, T_{ai}) = 0$. In our case, we have simplified the condenser as a straight tube where the flow configuration is countercurrent and the tube is divided into **M** cells. Therefore, the number of unknown variables is of order $\mathbf{5 \times M}$. Therefore, the solution can be obtained by the cell-by-cell method from the refrigerant inlet cell to the condenser outlet, thus starting with the superheated vapor model and then the two-phase vapor/liquid model and finally the liquid model.

The properties of the refrigerant in the inlet cell are known (see Table 1). However, the properties of the air and the wall temperature must be calculated separately (only in the first cell). Subsequently, the system of equations must be solved simultaneously for all cells following the inlet cell at each abscissa step. At each cell, we check the state properties of the refrigerant if they are at the saturation line, in other words, the conditions of transitions between the phases mentioned in paragraph (6). For this purpose, a threading of the enthalpy, temperature, and pressure profiles using the Vandermonde matrix and Toeplitz matrix method [8] has been included in the calculation code, the aim of which is to accurately determine the transition point between the states of the fluid. A simple flowchart illustrates the methodology of numerical resolution and is presented in Fig. 3.

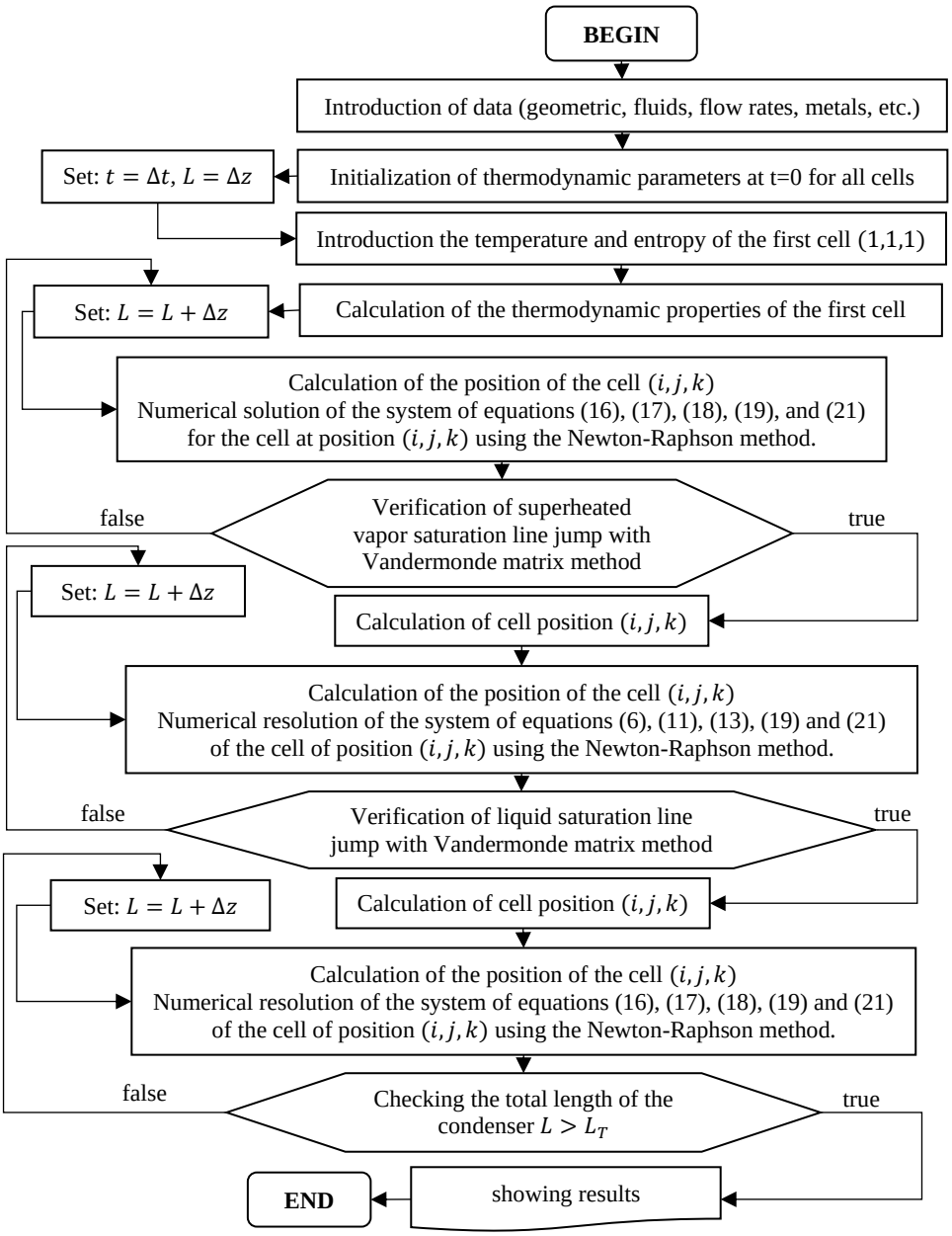

Fig.3. Flowchart of the numerical simulation of refrigerant flow in the condenser coil.

In this work, the Newton-Raphson algorithm has been used to solve this system of equations, and it is chosen for its stability, speed of convergence, and efficiency. Thus, the application of this method requires the calculation of the Jacobian matrix J and its inverse matrix J^{-1}, but this derivation procedure is more complicated, as in our case. To achieve this objective of numerical resolution of the

system of equations governing the flow of the three phases, we used the subroutines of Fortran Numerical Recipes [8]. The main subroutines that we used in our calculation code are mnewt, lubksb, ludcmp, usrfun, and fdjac. And on the other hand, we introduced in the calculation code the subroutines of Refprop V7.0 [23] which consist in calculating the different thermodynamic quantities $(\rho, h, P, x, \alpha, k, \mu, C_p, \sigma, etc\ldots)$. Consequently, the introduction of these subroutines makes the numerical resolution of the system of equations more flexible and easier to handle on a computer medium.

10. Results obtained

The results obtained from the numerical simulation are presented by profiles and show the evolutions of the thermophysical properties of the refrigerant, such as temperature, velocity, pressure, etc., respectively, along the condenser coil tubes under the fluid inlet conditions, i.e., the temperatures of the first coil cell of the condenser tubes at each instant. It is assumed that the gas compression in the compressor is isentropic $s = 1711.12\ kj/kg$, and the corresponding temperatures are indicated as follows:

Table (2). Initial conditions for temperature inputs into the condenser.

t **s**	***T*** **°C**	***t*** **s**	***T*** **°C**	***t*** **s**	***T*** **°C**
0.0	30	**1.0**	48	**2.0**	64
0.5	40	**1.5**	56	/	/

Figs (4), (5), and (6) represent the spatial variations of the density, temperature, and vapor quality of the refrigerant along the length of a tube (L) for an inlet temperature of 40°C at time $(t = 0.5s)$. It is noted that the profiles of temperature and vapor quality decrease with the increase in the stage number and the distance from the tube in the direction of flow and, vice versa for the density.

While figs. (7) to (9) show the temporal variations of the density, mass velocity, and heat transfer coefficient, respectively, of refrigerant along the length of the condenser tubes at different time steps (0.5, 1.0, 1.5, 2.0 s). In general, we note that quantities have significant values for high inlet temperatures. In addition, the density profile increases almost linearly in the superheated vapor phase and parabolically in the two-phase; on the other hand, in the liquid phase it remains practically stable, leading to the conclusion that the fluid in this state can be classified as an incompressible fluid.

Although the refrigerant heat transfer coefficient profile (Fig. 9.) shows moderate values in the superheated vapor phase, it presents considerable values in the two-phase compared to other phases. This demonstrates the importance of using refrigerants in refrigeration systems.

Thus, Fig. 10. shows the spatial variation of the fluid temperature along the coil tubes at $(t = 0.5\ s)$, Furthermore, the profile gradually decreases in a parabolic

manner in the superheated vapor phase and is nearly constant in the two-phase and decreases rapidly in the liquid phase. The purpose in this figure is to clarify the transition between the phases (superheated vapor, two-phase, liquid) using the method of the Vandermonde matrix and the Toeplitz matrix [25], which consists of finding the coefficients of the polynomial interpolation of the temperature variation in function of distance. This method is introduced in our calculation code.

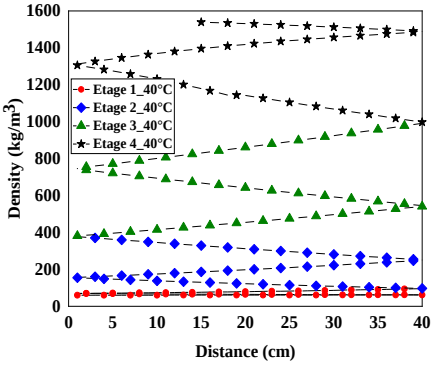

Fig. 4. Variation of the density along the coil (stages and columns) at t=0.5s.

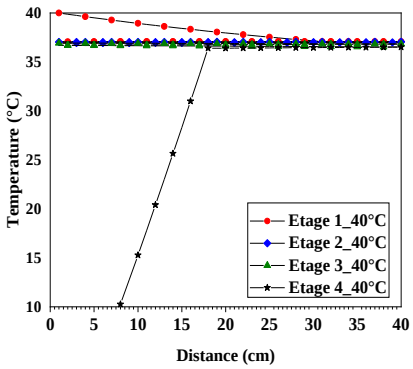

Fig. 5. Variation of temperature along the coil (stages and columns) at t=0.5s.

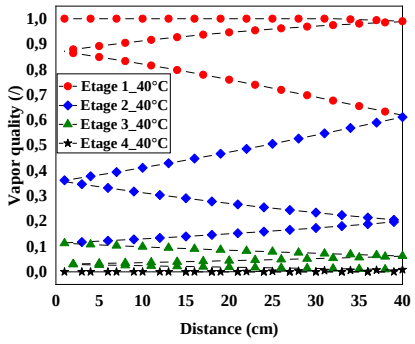

Fig. 6. Variation of vapor quality along the serpentine (stages and columns) at t=0.5s.

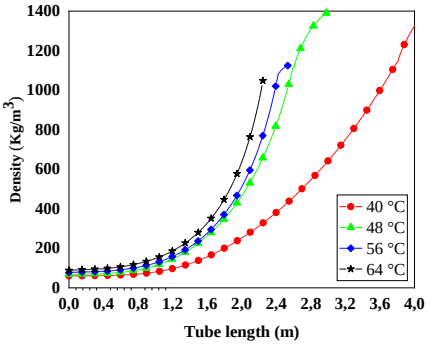

Fig. 7. Temporal variation of density along serpentine.

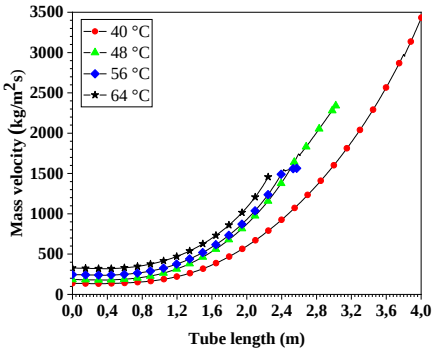

Fig. 8. Temporal variation of the mass velocity of the fluid along the serpentine.

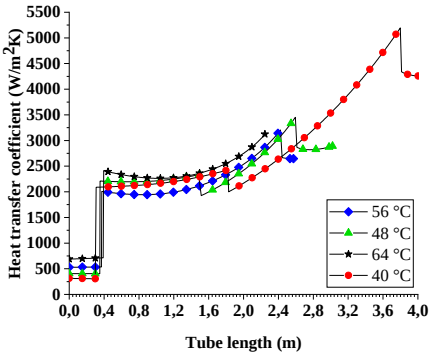

Fig. 9. Temporal variation of refrigerant heat transfer coefficient

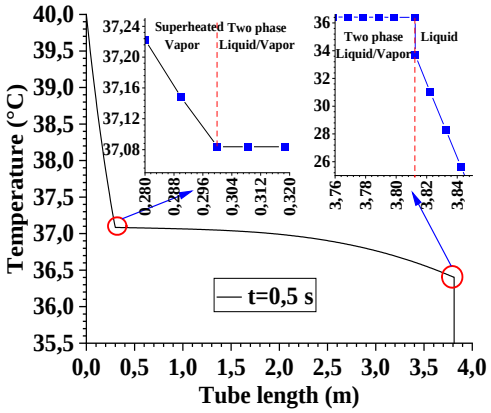

Fig. 10. Temperature profile at $t = 0.5s$ and the transitions between regions (superheated vapor/two phase/liquid).

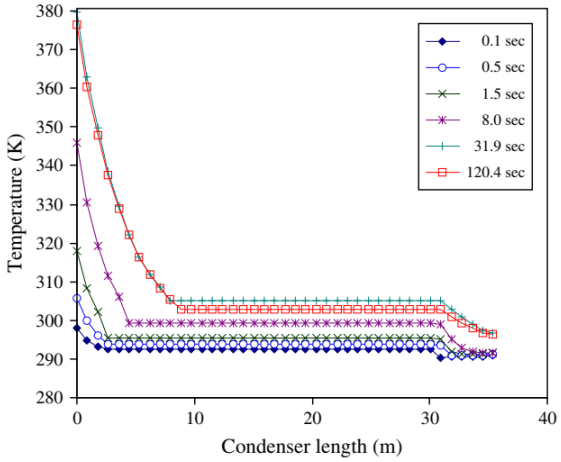

Fig. 11. The refrigerant temperature distribution in the condenser [7].

11. General conclusion

In this work, a numerical model has been developed describing the thermal and dynamic behaviors of a flow of refrigerant R22 inside the coil tubes of a compact condenser in an unsteady regime. The study is based on the principles of fluid mechanics and heat and mass transfer. The system of equations governing the flow inside the tubes is constituted by the equations of conservation of mass, momentum, and energy. Two other equations were considered, namely: the equation of the energy applied to the tube wall and the equation of the energy applied to the air. The parameters used in the system of equations and some correlations found in the literature were used to evaluate the friction force, the heat

transfer coefficient, the void fraction, and the viscosity of the fluid. The numerical methods used for solving the system of equations are mainly those of Newton-Raphson [25]. The model that we have developed proves useful in the design and optimization of refrigeration systems and also shows the advantage of using the Refprop V7.0 subroutines [23]. The graphical representation of the results obtained is in agreement with the results found in references [7, 21, 26] and as shown in Fig. 11 from a profile point of view. In the liquid region, the model of a compressible fluid was used, and the results obtained show that the density and the enthalpy are almost constant. Therefore, the model of an incompressible fluid is applicable in the liquid region.

Nomenclature

Latin alphabet

A_f Total surface area of the fins of an element per unit length [m^2 m^{-1}];
A_{to} Outer surface of tubes with collars and without fins of one element per unit length [m^2 m^{-1}];
A_o Total external surface area of the tube element per unit length [m^2 m^{-1}];
A_i Total internal surface area of the tube element per unit length [m^2 m^{-1}];
C_p Specific heat at constant pressure [$J.kg^{-1}K^{-1}$];
$C_{p,w}$ Specific heat at constant pressure of the tube wall [$J.kg^{-1}K^{-1}$];
D_o Outside diameter of the tube [m]; D_{to} Outside diameter of tube with collar [m];
D_i Inner diameter of the tube [m]; F^w Friction force on the wall [N m^{-3}];
F_k^{int} Momentum transfer at the interface resulting from viscous interfacial forces and pressure forces normal to the interface per unit volume [Nm^{-3}];
F_k^w Friction force between the tube wall and the phase k per unit volume [N m^{-3}];
f_x Resultant of frictional forces [N m^{-3}];
G Mass velocity [kg m^{-2} s^{-1}]; H Height of heat exchanger [m];
h_r Heat transfer coefficient of refrigerant [W m^{-2} K^{-1}];
h_0 Specific enthalpy [$J/kg^{-1}K^{-1}$]; h Total enthalpy [$J/kg^{-1}K^{-1}$];
J_s Colburn factor for dry air [/]; k Thermal conductivity [W m^{-1} K^{-1}];
L Total length of heat exchanger element [m];
l Total width of heat exchanger element [m];
M Mass [kg]. Spacing [m];
$M_{P,w}$ Mass of metal constituting the wall of the tube element [kg];
$\dot{m}$ Mass flow rate [kg s^{-1}]; P Pressure [N m^{-2}];
Pr Prandtl number [/]; $\backslash Q_r$
Heat flow exchanged between the refrigerant and the tube wall [W/m^2];
Q_a Heat flow exchanged between the tube wall and the outside air [W/m^2];
Q_w Heat flow in the wall [W/m^2];
s Entropy [$J/kg^{-1}K^{-1}$]; S_1 Vertical distance between tubes [center to center] [m];
S_2 Horizontal distance between tubes [center to center] [m];
T Temperature [K]; t Time [s]; t_c Fin collar thickness [m];
U Speed [m s^{-1}]; x Vapor Quality [kg kg^{-1}];
z Coordinated [m];
Δz_i Length of heat exchanger element [m];
Δz_j Vertical center distance of heat exchanger element [m];

Δz_k Longitudinal center distance of heat exchanger element [m];

Greek alphabet

α Void fraction; η_s Surface efficiency;
η_f Fin efficiency; ρ Density [kg m^{-3}];
Γ_{vl} Mass flow rate of vapor phase transferred to liquid phase per unit volume [$kgm^{-3}s^{-1}$];
Γ_{vl} Mass flow rate of liquid phase transferred to vapor phase per unit volume [$kgm^{-3}s^{-1}$];

Subscripts and exponents

a Air; f Friction; I Interface;
k Indicates the phase (liquid or vapor); L Liquid; V Vapor;
lv From liquid to vapor; vl From vapor to liquid; lo Liquid only;
vo Vapor only; w Tube wall; r Refrigerant; row Tube Row;
s Exit from the tube; or single phase; to Outer side of tube wall with collar;
wL From the tube wall to the liquid refrigerant;
wV From the tube wall to the vapor refrigerant;
sat Saturation; w Wall.

R E F E R E N C E S

[1] *Xiang Dong He, Sheng Liu, Haruhiko Asada, Cristian Cuevas, Jean Lebrun, Vincent Lemort, Philippe Ngendakumana*, Development and validation of a condenser three zones model, Applied Thermal Engineering Vol.29, pp. 3542-3551, 2009

[2] *M. Willatzen, N. B. O. L. Pettit and L. Ploug-Sørensen*, A general dynamic simulation model for evaporators and condensers in refrigeration. Part I: moving-boundary formulation of two-phase flows with heat exchange, Int J. Refrig. Vol. 21, No. 5, pp. 398-413, 1998.

[3] *M. Willatzen, N. B. O. L. Pettit and L. Ploug-Sørensen*, A general dynamic simulation model for evaporators and condensers in refrigeration, Part II: simulation and control of an evaporator, Int J. Refrig. Int J. Refrig. Vol. 21, No. 5, pp. 404-414, 1998.

[4] *Conditions Xing Xuea, Xianming Fenga, Junmin Wanga, Fang Liua*, Modeling and Simulation of an Air-cooling Condenser under Transient, International Conference on Advances in Computational Modeling and Simulation, Procedia Engineering Vol. 31, pp. 817-822. 2012.

[5] *X. Jia, C. P. Tso and P. K. Chia*, A distributed model for prediction of the transient response of an evaporator, Int. J. Refrig. Vol. 18, No. 5. pp. 336-342, 1995.

[6] *H. Wang and S. Touber*, Distributed and non-steady-state modelling of an air cooler, Int. J. Refrig., vol. 14, No. 2, pp. 98-111, 1991.

[7] *F.Q. Wang, G.G. Maidment, J.F. Missenden, R.M. Tozer*, A novel special distributed method for dynamic refrigeration system simulation, Int. J. Refrig, Vol. 30, pp. 887-903, 2007.

[8] *Saul A. Teukolsky, William T. Vetterling, P. Flannery Frontmatter*, Numerical Recipes: The Art of Scientific Computing, Cambridge University Press, Third Edition.

[9] *X. Jia, C. P. Tso, P. Jolly, and Y. W. Wong*, Distributed steady and dynamic modelling of dry-expansion evaporators, Int. J. Refrig., vol. 11, pp. 126-136, 1999.

[10] *S. Mostafa Ghiaasiaan*, Two-phase flow, boiling and condensation: In conventional and miniature systems, Published in the United States of America by Cambridge University Press, New York, 2007.

[11] *John R Thome*, Encyclopedia of Two-Phase Heat Transfer and Flow I and II, Publisher: World Scientific Publishing Company, September 1, 2015.

[12] *Mamoru Ishii, Takashi Hibiki*, Thermo-Fluid Dynamics of Two-Phase Flow, Second Edition Springer, 2011.

[13] *Demba Ndiaye, Michel Bernier*, Transient Modeling of Refrigerant-to Air Fin-and-Tube Heat Exchangers, American Society of Heating, Refrigerating and Air-Conditioning Engineers, HVAC&R Research Vol. 16, Issue 3, May 2010.
[14] *Yang Yao, Yiqiang Jiang, Shiming Deng, Zuiliang Ma*, A study on the performance of the air side heat exchanger under frosting in an air source heat pump water heater/chiller unit, Int. J. of Heat and Mass Transfer, Vol. 47, pp. 3745-3756, 2004.
[15] *F.C.McQuiston ,D. Jerald, D. Parker Jeffrey*, Heating, Ventilating, and Air Conditioning Analysis and Design, John Wiley & Sons, Inc. Sixth Edition 2005.
[16] *J. R. Thome*, Engineering Data Book III, in Wolverine tube, Inc, 2006.
[17] *N. Kayansayan Dokuz Eylfil*, Heat transfer characterization of plate fin-tube heat exchangers, Int. Froid Vol. 17 No 1, 1994.
[18] *N. Kayansayan*, Heat Transfer Characterization of Flat Plain Fins and Round Tube Heat Exchangers Experimental Thermal and Fluid Science. Elsevier Science,1993.
[19] *Pallippattu Krishnan Vijayan Arun Nayak Naveen Kumar*, Single-phase, Two-phase and Supercritical Natural Circulation Systems. Woodhead Publishing, 2019.
[20] *Reinhard Radermacher, Yunho Hwang*, Vapor Compression Heat Pumps with Refrigerant Mixtures CRC, Press Taylor & Francis Group 2005.
[21] *O. Garcıa-Valladaresa, C.D. Perez-Segarrab, J. Rigola*, Numerical simulation of double-pipe condensers and evaporators, Int. J. Refrig, Vol. 27, pp. 656-670, 2004.
[22] J. R. Figueiredo, R. G. Santos, C. Favaro, A. F. S. Silva, A. Sbravati, Substitution-Newton-Raphson method applied to the modeling of a vapour compression refrigeration system using different representations of the thermodynamic properties of R-134a, J. Braz. Soc. Mech. Sci. Vol.24, No.3 Rio de Janeiro jul 2002.
[23] *E.W. Lemmon, M.L. Huber, M.O. McLinden*, Reference fluid thermodynamic and transport properties REFPROP, Standard Reference Database 23, version 8.0. NIST, U.S. secretary of commerce on behalf of the United States of America, 2007.
[24] EgiChem laboratory CICECO – Aveiro Institute of Materials in the University of Aveiro (Portugal). Properties of dry air at atmospheric pressure, Site web: https://www.egichem.com/tools/calculators/air-properties/
[25] *Xiangdong He, Sheng Liu, Haruhiko Asada*, Modeling of Vapor Compression Cycles for Advanced Controls in HVAC Systems, Proceedings of the American Control Conference Seattle, Washington, June 1995.
[26] *J. W. MacArthur, E. W. Grald*, Unsteady compressible two-phase flow model for predicting cyclic heat pump performance and a comparison with experimental data, Int. J. Refrig., Vol. 12, pp. 29-41, 1989.